

## Impact of cement content in cement bound materials on the reflection cracking performance of asphalt pavements

Debby Marcelia Andryanti <sup>a</sup>, Tam Minh Phan <sup>a</sup>, Dong-Wook Lee <sup>b</sup>, Dae-Wook Park <sup>a,\*</sup>

<sup>a</sup> Dept. of Civil Engineering, Kunsan National University, 558 Daehak-ro, Gunsan-si, Jeonbuk-do 54150, the Republic of Korea

<sup>b</sup> Dept. of Civil Engineering, Jeju National University, 102 Jejudaehak-ro, Jeju, the Republic of Korea

### ARTICLE INFO

**Keywords:**

Cement bound material  
Thermal coefficient expansion  
Reflection cracking  
Pavement design

### ABSTRACT

This study investigates the impact of cement contents in cement bound material (CBM) on asphalt pavement reflection cracking, considering two levels: 4.5 % (CBM1) and 5.4 % (CBM2). Mechanical properties of CBMs, including elastic modulus, rupture modulus, and thermal expansion, were evaluated. Simultaneously, properties of asphalt pavement layers (wearing course and base course) underwent assessment through dynamic modulus, flow number, and overlay tests. Resilient modulus tests were conducted for subbase and subgrade layers. Laboratory test outcomes served as inputs for a AASHTOWare Pavement ME Design program. The results indicated that despite CBM2's higher elastic modulus and rupture modulus, CBM1 outperformed in pavement design. Based on the outcomes from pavement design program CBM1 exhibited lower total transverse cracking (400.19 m/km) compared to CBM2 (403.38 m/km) after 6 years of service. The higher cement content in CBM2 was identified as a potential contributor to increased cracking, attributed to shrinkage during cement hydration process. Moreover, the higher cement content showed a higher coefficient of thermal expansion (CTE), where CBM1 displayed a CTE of 70  $\mu\text{m}/^\circ\text{C}$ , while CBM2 material had a CTE of 40  $\mu\text{m}/^\circ\text{C}$ . These findings emphasize the intricate relationship between cement content in CBM and pavement performance, crucial for effective design considerations.

### 1. Introduction

High-quality road infrastructure plays a crucial role in the economic development and growth of any country. As the number of vehicles on the roads increases, the demand for efficient road systems grows [1]. Currently, asphalt pavement with cement bound material (CBM) is widely favored for high-grade highways due to its numerous advantages, including high strength, stiffness, smoothness, anti-fatigue performance, and cost effectiveness [2]. Utilizing CBM in pavement layers has emerged as an alternative design and construction solution. To make soils suitable for subbase and base layers, they are modified or stabilized with cement. CBM is typically created by mixing granular material or soil with cement and compacting it at or near optimum moisture content using external vibration. The mix design for CBM is carefully conducted to achieve the desired strength and stability. This results in a stiffer and stronger base compared to an unbound aggregate base [3]. Tataranni et al. conducted a test bed using a 100 % Recycled Cement Bound Mixture (RCBM) for the base layer. Their findings showed that RCBM is a viable option for constructing base layers, delivering appropriate performance [4]. However, the cement-stabilized base can be susceptible to transverse crack issues caused by drying

\* Corresponding author.

E-mail address: [dpark@kunsan.ac.kr](mailto:dpark@kunsan.ac.kr) (D.-W. Park).

shrinkage and low-temperature shrinkage during its strength formation. Hassan et al.'s study suggested that CBM can enhance strength but may also raise the risk of reflection cracking in the asphalt overlay in Qatar [5]. In addition, the repeated action of heavy traffic loads can lead the stress concentration at the crack tips, causing further cracking that soon form and even up to the asphalt surface, a phenomenon known as reflective cracking. Reflective cracking is associated with existing pavement cracks and joints and usually extends from the bottom to the surface of pavements under traffic load or thermal expansion and contraction [6]. After the reflective crack up to the surface of the pavement, the pavement will be roughened and moisture will penetrate to the interior of the pavement structure, causing the pavement to deteriorate quickly [7]. These surface cracks may not severely impact the structural bearing capacity of the composite pavement when narrow (less than 3 mm). Nevertheless, wider cracks can lead to water infiltration, accelerating structural pavement failure, weakening the strength and stability of the subgrade, and ultimately reducing the pavement's lifespan.

Crack space in a cement-stabilized base can vary due to multiple factors. Generally, the transverse cracks can be divided into two categories: the reflection crack (R-crack), developing from the transverse crack in CBM up to surface layer, and the temperature shrinkage cracks (T-crack), developing from up to down but they are almost the same forms on pavement surface in sight [8]. Shrinkage of CBM possibly due to (a) moisture changes, which result in surface and capillary tension, movement of interlayer water and disjoining pressure and (b) chemical reactions (hydration/dehydration shrinkage, thermal shrinkage, crystallization swelling, carbonation shrinkage and phase transition shrinkage) [9]. Drying shrinkage is the reduction in volume caused principally by the loss of water during the drying process. In some cases, volume changes due to chemical reactions influence porosity and degree of saturation. The volume changes induced by chemical processes are influenced by temperature. This is because an increase in temperature typically accelerates chemical reactions, while a decrease in temperature has the opposite effect, slowing down these reactions [10]. The assumption is made that shrinkage tends to reach a stable value as time approaches infinity. This stabilization is conditional upon various factors that impact the drying process of concrete. These factors encompass relative humidity and temperature, the mix characteristics (in particular, the type and amount of binder, water content and cement ratio, and the type of aggregate), and the size as well. Several factors encompass the material characteristics which influenced the drying shrinkage, especially cement content that play key roles in CBM. Interestingly, there were some cases where soils exhibit volume change without cement, increasing the cement content actually reduces total shrinkage [11]. However, excessive cement content can lead to higher water consumption during hydration process, causing an increase in drying shrinkage. The cement content is the most important factor affecting the temperature shrinkage. With increasing cement content, the average temperature shrinkage coefficient also increases [12]. Furthermore, increase in cement content potentially leads to enlarged rigidity and excessive strength. While higher tensile strength causes cracks to be spaced farther apart when the material still undergoes the same amount of shrinkage as a material with lower cement content, resulting in wider cracks. Shrinkage was initially reduced with a small amount of cement addition but steadily increases with higher cement content. Therefore, to minimize the impact of cement content on shrinkage, it is crucial not to exceed the cement content for adequate durability.

Previous research has primarily focused on studying reflective cracking in asphalt pavement caused by traffic loading. Hu et al., recently investigated thermal reflective cracking from a classical fracture mechanics perspective; however, their analysis was limited to mainly brittle materials. In general, asphalt pavement deformation influenced by factors such as traffic loading, climate conditions, and the conditions of the base and subgrade [13]. Highway design manuals commonly assess the strength of road subgrade using the California Bearing Ratio (CBR), which depends on the soil type, density, and moisture content. To accurately classify the strength of the subgrade, field studies were conducted. Given the prevalence of soils in the area, using a single subgrade modulus for the entire road stretch is a major concern. Considering the potential variability of the subgrade modulus is recommended. Recently, researchers have explored functional layers to prevent crack propagation through laboratory and field tests [14]. Laboratory tests are effective tools for examining material characteristics and facilitating the understanding of crack initiation and propagation phenomena. While several studies have explored the impact of CBM on pavement performance, there remains a notable gap in research evaluating the influence of cement content on CBM material properties such as shrinkage and thermal expansion. Furthermore, little attention has been given to evaluate the effect of CBM properties on the performance of pavements constructed with CBM.

Therefore, the current study aims to analyze the material characteristics of CBM across varying cement contents, includes assessing the impact of CBM characteristics on the formation of reflective cracking in asphalt layers. The tests comprised an assessing elastic modulus test, and flexural strength test of CBM. Through comparative analysis of the test, it is helped to find CBM behavior in different cement content. The dynamic modulus, flow number test, and overlay test of the asphalt mixtures (e.g., wearing, and base course), and resilient modulus of the subbase and subgrade was also conducted. In addition, a parameter study exploring the potential variability of subgrade modulus was taken into consideration. The material characteristic properties of CBM and asphalt mixtures were then used to simulate a pavement model using a AASHTOWare Pavement ME Design program. The most effective pavement model was determined to be used as the connecting road between Al Faw Grand Port and Um Qasr in Iraq.

## 2. Materials and test methods

### 2.1. Cement bound material (CBM)

Materials for sample preparation were sourced from the region between Al Faw Grand Port and Um Qasr in Iraq and sieved into three different sizes based on ASTM C 39 standard [15]. The aggregates consisted of 32 mm, 14 mm, and fine materials. Ordinary Portland Cement Type 1 (OPC) was used as the binder for Cement Bound Material. Following the guidance from earlier studies and trial tests conducted in the laboratory to ascertain the optimal cement content, the evaluation of the cement content's effects focused on two specific concentrations. CBM1 featured a 4.5 % cement content, while CBM2 incorporated 5.4 % cement content, both expressed as a

percentage of the total mixture's weight. The CBM mixture proportions are presented in [Table 1](#).

## 2.2. Asphalt mixture

Asphalt binder PG 76-10 and PG 70-10 were respectively employed for the wearing and base courses, respectively. The properties of two asphalt binders are displayed in [Table 2](#) and [Table 3](#). The wearing course mixture consisted of three types of aggregate – 19 mm, 8 mm, and 5–0 mm, while the base course mixture incorporated four types of aggregate – 32 mm, 19 mm, 8 mm, and 5–0 mm as shown in [Fig. 1](#). The designed aggregate gradation for the wearing and base course can be seen in [Table 4](#) and [Table 5](#). The properties of two mixture design are shown in [Table 6](#).

## 2.3. Subbase and subgrade

The subbase and subgrade material shown in [Fig. 2](#). The optimum water content for the subbase and subgrade was determined using the methods outlined in the “Methods of test for soils for civil engineering purposes” (BS 1377 part 4) [16]. The findings indicate an optimal water content of 7.0 % by weight for subbase and 8.4 % by weight for subgrade ([Fig. 3](#)).

## 2.4. Test methods of CBMs

Two primary tests were conducted on CBM to assess their properties, included elastic modulus test, and flexural strength test as shown in the [Table 7](#). For each mixture, three replicates were prepared. The results obtained from the elastic modulus test and flexural strength test serve as crucial inputs for the pavement design program.

### 2.4.1. Elastic modulus test

The elastic modulus measured based on ASTM C39 using the compressometer. A cylinder sample with 200 mm height and 100 mm in diameter was compacted using a hand compactor and cured in a moisture oven for 28 days before testing. The load was applied continuously at a rate of 0.25 mm/min without interruption, and the stress and strain were recorded. The objective of the elastic modulus test was to measure the CBM stiffness and evaluate its mechanical properties, as the sample underwent compressive strength analysis according to [Eq. \(1\)](#).

$$C = \frac{P}{A} \quad (1)$$

Where:

C: Compressive strength (Pa).

P: Peak load (N).

A: Surface area ( $\text{m}^2$ ).

The elastic modulus of CBM materials was investigated using the stress-strain relationship of the mixture from the test. The elastic modulus (E) is calculated by [Eq. \(2\)](#).

$$E = \frac{\text{Stress}}{\text{Strain}} \quad (2)$$

### 2.4.2. Flexural strength test

CBM flexural strength was determined following the guidelines of ASTM C 78 [17]. A third-point test configuration was employed on beam samples with dimensions of 400 mm in length, 100 mm in depth and width. The load was applied by two rollers connected to the head of the bending machine, with a loading rate of 0.05 mm/min. Throughout the testing process, both the load and displacement were recorded. The modulus of rupture was calculated using the [Eq. \(3\)](#).

$$R = \frac{4P}{bd^2} \quad (3)$$

Where:

R: Modulus of rupture (Pa).

P: Ultimate load taken from the test (N).

a: Average distance between line of fracture and the nearest support measured (m).

b: Average width at the fractured face (m).

**Table 1**

CBM materials mixture proportions (kg).

Sample	Cement (OPC)	Water	32 mm	14 mm	Fine Agg
CBM1	103.0	161.4	519.5	290.9	1267.6
CBM2	123.0	155.6	517.0	289.5	1261.5

**Table 2**  
Properties of PG 76-10 binder.

Test description	Specification limit	Result
(Original) G*/sinδ @76 °C	≥ 1.0 kPa	3.37
(RTFOT) G*/sinδ @76 °C	≥ 2.2 kPa	5.34
G* sinδ at 10 rad/s @37 °C	≤ 5000 kPa	937
(PAV) Creep Stiffness (S) @0 °C	≤ 300 MPa	71.5
(PAV) m-Value @0°C	≥ 0.30	0.334

**Table 3**  
Properties of PG 70-10 binder.

Test description	Specification limit	Result
(Original) G*/sinδ @70 °C	≥ 1.0 kPa	1.14
(RTFOT) G*/sinδ @70 °C	≥ 2.2 kPa	2.46
G* sinδ @34 °C	≤ 5000 kPa	2102
G* sinδ @31 °C		3110
(PAV) Creep Stiffness (S) @0 °C	≤ 300 MPa	42.218
(PAV) Creep Stiffness (S) @-6 °C		105.54
(PAV) Creep Stiffness (S) @-12 °C		216.142
(PAV) m-Value @0 °C	≥ 0.30	0.4174

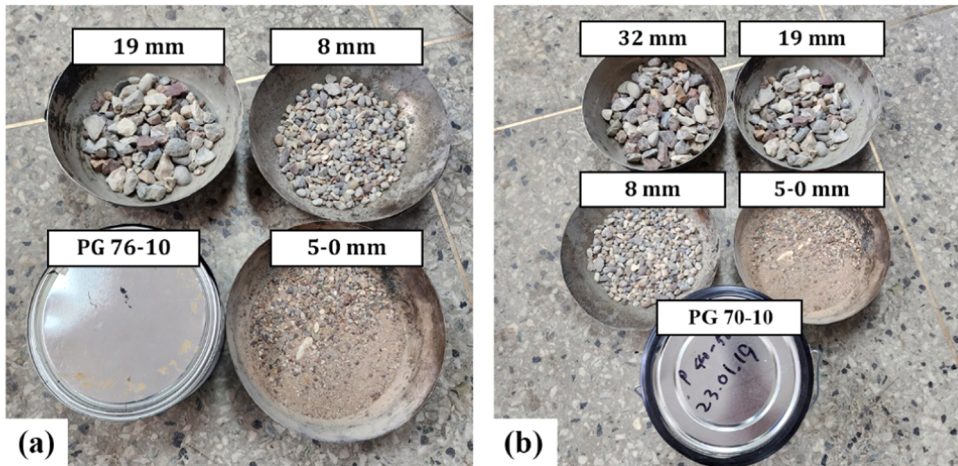


Fig. 1. Aggregates and binder used in (a) wearing course and (b) base course asphalt mixture.

**Table 4**  
Aggregate gradation of asphalt wearing course.

Sieve size (mm)	Passing percentage (%)									
	19	12.5	9.5	4.75	2	1.35	0.6	0.25	0.125	0.075
Design	100	78–90	71–83	59–71	44–56	39–47	29–37	14–22	5–13	5–8
Use	100	87.9	81.7	45.8	45.8	39.6	30.2	18.4	9.2	6.6

**Table 5**  
Aggregate gradation of asphalt base course.

Base course Sieve size (mm)	Passing percentage (%)									
	37.5	25	19	12.5	9.5	4.75	2	0.425	0.18	0.075
Design	-	100	92–100	82–95	75–92	60–82	42–70	20–45	10–28	3–10
Use	-	94.2	83.8	72.2	66.1	44.8	28.1	14.8	7.3	4.0

**Table 6**  
Design criteria for marshall design mixes.

Properties	Wearing	Base course
Binder content, %	5.3	4.2
Maximum Theoretical Specific Gravity ( $G_{mm}$ )	2.397	2.436
Bulk specific gravity ( $G_{mb}$ )	2.301	2.317
Voids in total mix (VTM), %	4.0 (3 ÷ 5)	4.9 (3 ÷ 7)
Voids in mineral aggregate (VMA), %	15.8 (12 ÷ 14)	14.2 (12 ÷ 14)
Void fill with asphalt (VFA), %	74.8 (70 ÷ 85)	62.9 (60 ÷ 80)
Stability, kN	18.86 (> 9)	13.83 (> 6)
Flow, mm	2.31 (2 ÷ 4)	2.96 (2 ÷ 5)



Fig. 2. Aggregates of (a) subbase and (b) subgrade.

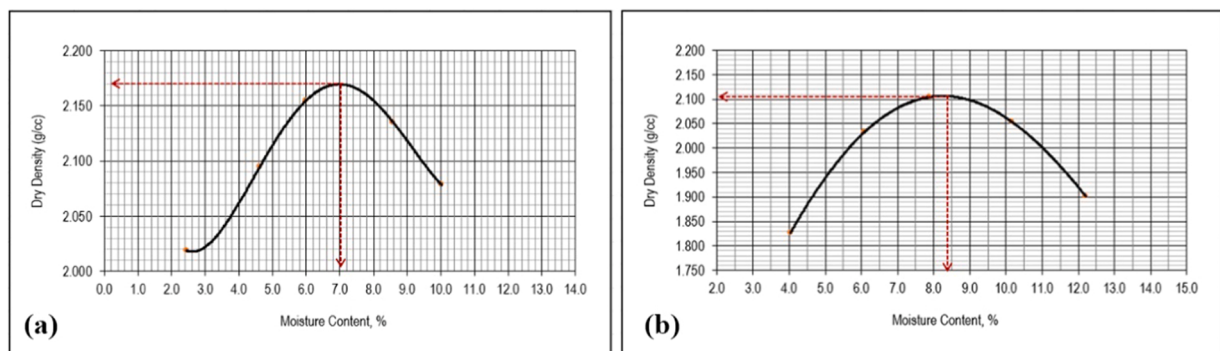


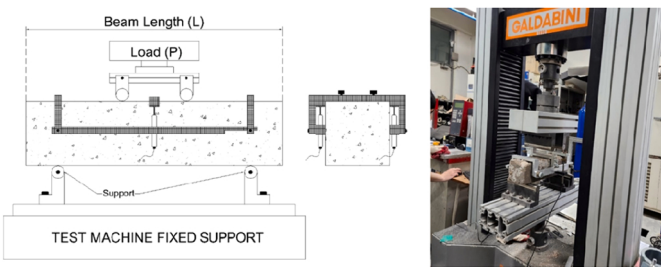
Fig. 3. Maximum dry density and optimum water content of (a) subbase and (b) subgrade.

d: Average depth at the fractured face (m).

#### 2.4.3. Coefficient of thermal expansion

To evaluate the drying shrinkage in CBM, coefficient of thermal expansion (CTE) was performed. The CTE of cement bound materials has not been previously measured on a national level, and no standardized test procedure currently exists for its measurement. Therefore, the author team developed a straightforward method using available tools. Cement bound material to approximately 200 mm in length and 100 mm in diameter with a double blade saw and attached two metal studs to each end surface. After placing the samples in a temperature chamber for 24 h, they measured the distance between the two ends with a high-resolution caliper. The process was repeated for five additional temperatures: 0, 15, 25, 35, and 50 °C.

**Table 7**  
CBM test procedure.

Test	Test standard	Test procedure
Elastic modulus	ASTM C39 [15]	
Flexural strength	ASTM C78 [17]	
Coefficient of thermal expansion (CTE)	-	

## 2.5. Test methods of asphalt mixtures

A comprehensive evaluation of the properties in the wearing course and base course was conducted by implying three laboratory tests. These comprised dynamic modulus test, flow number test, and overlay test (OT) as shown in the Table 8. Through the testing it helps to understand the properties of both mixtures for the purpose of pavement design.

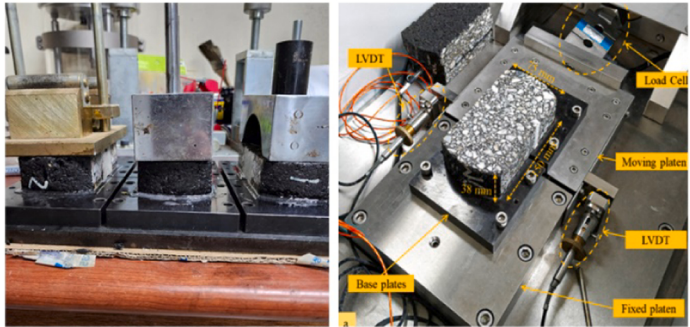
### 2.5.1. Dynamic modulus test

Dynamic modulus is a critical indicator of the asphalt mixture's stiffness, evaluated through a compressive-type, repeated load test. In the Mechanistic-Empirical Pavement Design Guide (MEPDG) [20], dynamic modulus plays a significant role in predicting rutting and fatigue cracking distress. Test samples with a height of 150 mm and a diameter of 100 mm were meticulously prepared in accordance with the requirements. The hot-mix asphalt (HMA) test samples were compacted of  $7 \pm 1\%$ . To explore the impact of different temperatures, the experiment encompassed four testing temperatures:  $-10^\circ\text{C}$ ,  $4^\circ\text{C}$ ,  $21^\circ\text{C}$ , and  $37^\circ\text{C}$ . For each temperature, six frequencies were conducted, including 25 Hz, 10 Hz, 5 Hz, 1 Hz, 0.5 Hz, and 0.1 Hz. The applied load for each frequency was based on AASHTO T342-11 guidelines [18].

### 2.5.2. Flow number test

The flow number test serves as a straightforward performance evaluation method, specifically related to rutting resistance of HMA mixture [21]. The specimens used for the Flow Number test had dimensions of 150 mm in height and 100 mm in diameter. Initially, these samples underwent a 2-hour preconditioning in an incubator at  $54^\circ\text{C}$  to achieve the desired temperature. The Flow Number test involved dynamic creep testing, employing a haversine-type loading pattern with intervals of rest between loadings. In this study, the test was conducted under conditions of unconfined pressure and 0.7 MPa compressive stress. The testing chamber was allowed to stabilize at the testing temperature of  $54^\circ\text{C}$  for a minimum of one hour. Each loading cycle comprised a 0.1-s load period followed by a 0.9-s rest period. The test concluded either after 10,000 cycles or upon reaching a five percent permanent strain.

**Table 8**  
Asphalt mixture test procedure.

Test	Test standard	Test procedure
Dynamic modulus	AASHTO T342-11 [18]	
Flow number	AASHTO T342-11 [18]	
Overlay test (OT)	Tex-248-F-09 [19]	

### 2.5.3. Overlay test

The overlay test (OT) method has proven to be a reliable and practical approach for screening and evaluating the crack resistance of HMA in laboratory settings [22]. Zhou [23] utilized the OT to evaluate the fracture properties of laboratory mixed laboratory compacted asphalt specimens based on the Paris' law. The shape of the crack growth function was approximated by the load history, and the magnitude was calibrated to monitoring by a digital camera. The stress intensity factor for a recorded crack length was computed. With the crack growth function and stress intensity factor being known, the fracture properties were finally determined from regression analysis. OT is designed to assess the susceptibility of bituminous mixtures to fatigue or reflective cracking by measuring the number of cycles to failure. Through this method, the sample's critical fracture energy parameter and resistance index are determined. The test was conducted following the Tex-248-F-09 procedure [19]. Before testing, the sample was conditioned at 25 °C for a minimum of one hour and maintained at  $25 \pm 0.5$  °C throughout the test. Continuous loading was applied at a controlled rate of 10 s per cycle until the peak load was reduced by at least 93 percent relative to the initial cycle's peak load. In cases where 1200 cycles are conducted without reaching the 93-percent reduction, the test is terminated [22,24].

### 2.6. Test methods of subbase and subgrade

The resilient modulus of both the subbase and subgrade was tested in accordance with AASHTO T 307 [25]. The subbase and subgrade samples were prepared with optimum water content of 7.0 % by weight for subbase material and 8.4 % by weight for subgrade material. Various loading sequences of deviatoric stress and confining pressure were applied during the testing. The deviatoric stress, resilient deformation, and permanent deformation were recorded for the final five cycles of each loading sequence. The sample testing was terminated if the permanent deformation exceeded 5 percent of the sample height, as specified by AASHTO T

307. Additionally, for a conservative approach and parametric study, the possible variability of the subgrade modulus was taken into consideration. The parametric study was calculated using the back calculated Eq. (4). The parameter ( $\alpha$ ) of possible subgrade modulus ranged from 0.8 to 0.95 with step of 0.05.

$$M_R = \alpha M_{R(measured)} \quad (4)$$

## 2.7. Pavement design

To meet the objective to assess the impact of cement content for reflective cracking, a pavement model was simulated using pavement design program. The evaluation comprises fatigue cracking, transverse cracking, thermal cracking, and top-down cracking to gain comprehensive insights into CBM's viability throughout the pavement's service life [26]. The AASHTOWare Pavement ME Design program incorporates various inputs, such as the properties of layer materials (surface course, base course, cement bound material, subbase, and subgrade), traffic level, weather conditions, and the desired design life. Utilizing mechanistic-empirical calculations, the program generates outputs including terminal International Roughness Index (IRI), overall asphalt concrete cracking, rutting, and the projected performance life of the designed pavement. In this study, two pavement designs with CBM alternatives shown in Fig. 4. The pavement structures used in this study included two courses of asphalt (wearing course and base course), base,

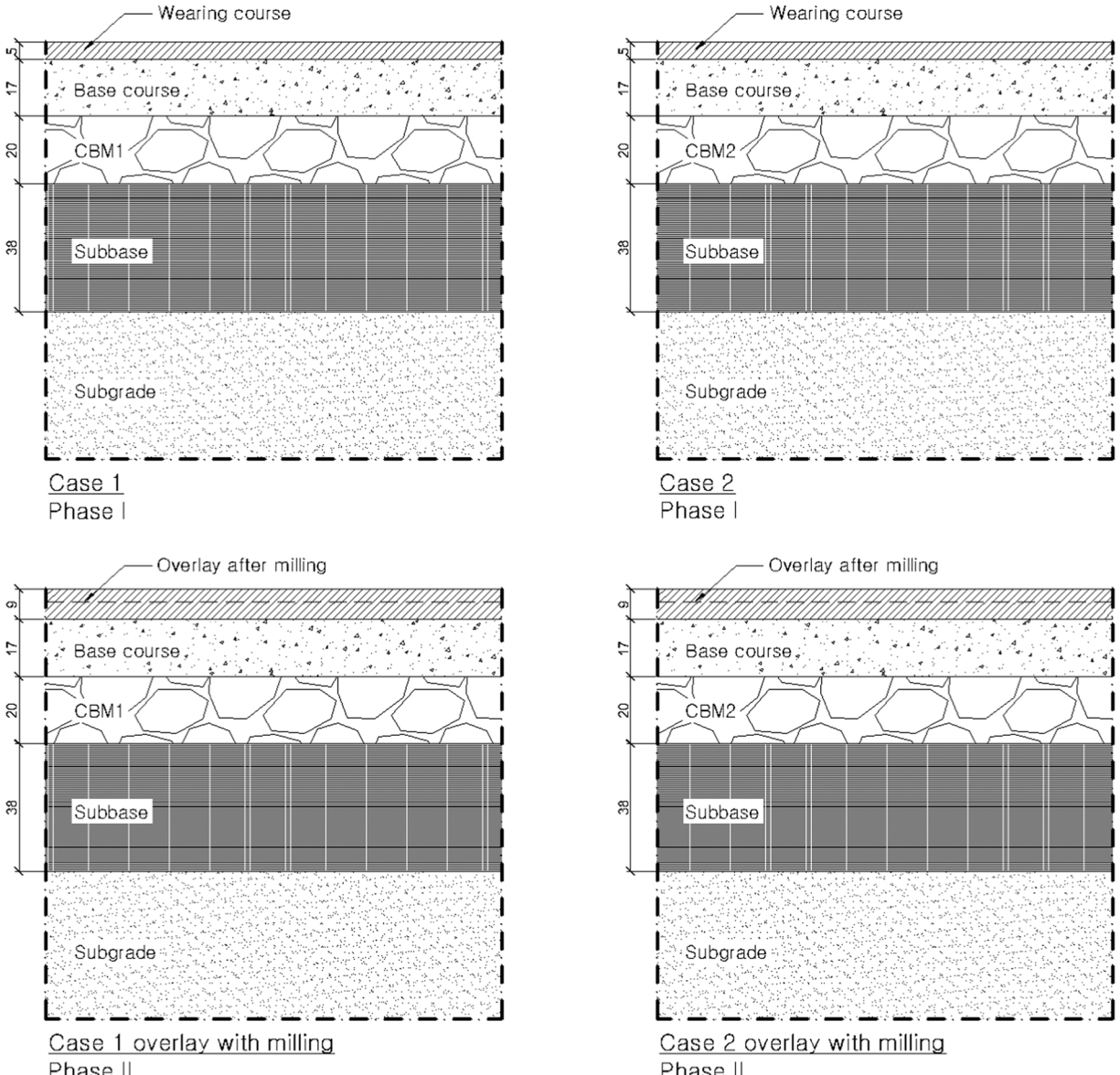


**Fig. 4.** Cases of pavement model in Phase I and Phase II (overlay with milling).

subbase, and subgrade. The pavement model was examined with two-phase analysis was implied. During Phase I, the primary emphasis is on designing a new pavement design, with a specific goal of achieving a minimum pavement lifespan of 6 years. Following this, the next step involves milling, and a 9 cm overlay will be implemented in Phase II of the pavement design. This was taken to mitigate cracking caused by the increase in vehicle volume, with the objective of ensuring a minimum pavement lifespan of 14 years.

The traffic input was considered as truck only (Annual Average Daily Traffic of Truck-AADTT) reflecting the real traffic condition on the connecting road between Al Faw Grand Port and Um Qasr in Iraq. The total AADTT is 14,161 veh/day, consisting of two types of trucks: 4-axis and 5-axis, with proportion of 60 % and 40 % respectively. For each model, two traffic volume inputs were chosen: Phase I represent 30 % of the total traffic volume, and Phase II represent 70 % of the total traffic volume. The traffic volume detail is provided in [Table 9](#).

Incorporating environmental factors is a crucial aspect of the Mechanistic-Empirical (ME) pavement design program, especially when considering the response of pavement distress prediction to climate inputs. An evaluation of flexible pavement using MEPDG revealed the sensitivity of asphalt pavement performance to climate changes [27]. The climate data was applied using the Iraq location's latitude and longitude. The program utilizes climate data based on the Federal Highway Administration LTPP (Long-Term Pavement Performance) sites.

### 3. Results and discussions

#### 3.1. Elastic modulus of CBM

[Fig. 5](#) presents the compressive strength and elastic modulus of CBM. The study investigated the elastic modulus of CBM materials using the stress-strain relationship of the mixtures as shown in [Fig. 6](#). According to a study by Hanifa [28], typical stabilized bases with a 28-day curing period have elastic modulus value ranging from 1000 to 2000 MPa, indicating a stiffer mixture with higher elastic modulus values. The figure clearly demonstrates that for each property the effect of cement content can be quite different. Comparatively, CBM1 with a lower cement content generally exhibited lower results than CBM2 in elastic modulus, which was 1711 MPa. CBM2, with an average elastic modulus of 2189 MPa after a 28-day curing period, exceeded the generally observed modulus value range. These trends suggest that the effect of cement content in elastic modulus can also be influenced by aggregate materials and water content [29].

#### 3.2. Flexural strength of CBM

[Fig. 7](#) shows the rupture modulus of CBM. The flexural tensile strength of concrete is an important parameter for designing the flexure members. The effect of cement content on elastic modulus also mirrored the findings of the flexural strength test results, where an increase in cement content correlated with an increase in the ratio of flexural strength. It observed that CBM2 with 0.9 % higher cement content exhibits 0.929 MPa of rupture modulus. Meanwhile rupture modulus in CBM1 shows 39 % lower. This is possibly because the larger size of laterite particles not well compacted [30]. From Karihaloo's theory [31], the difference in aggregate proportions also contribute to the observed variations in flexural strength between CBM1 and CBM2. Additionally, the age of cement-stabilized will influence the mechanical properties of concrete including its rupture modulus. The flexural strength increases with increase of age and strength of concrete. The proportional increase in the flexural tensile strength at same age of concrete strength [32].

#### 3.3. Coefficient of thermal expansion

[Fig. 8](#) shows the CTE results of CBM. Through linear interpolation, the CTE was determined. It is evident that CBM1 containing 4.5 % of cement content exhibits lower strains compared to CBM2 with 5.4 % of cement content. The findings indicate that CBM1 has a CTE of  $70 \mu\text{m}/^\circ\text{C}$ , while CBM2 material had a CTE of  $40 \mu\text{m}/^\circ\text{C}$ . The CTE of CBM decreased due to the reducing cement content in the mixture. The difference might be because the CBM experience significant temperature rise due to the heat of hydration causing the material to experience thermal stress. In addition, the increase in CTE can be explained by the effect of internal water pressure as it explained by Siddiqui et al. [33]. Study from Mallela et al. [34] and Tanesi [35] mentioned that CTE significantly affected pavement performance. The higher CTE of cement bound material potentially caused the more chance of reflective cracking in asphalt pavement.

#### 3.4. Dynamic modulus

[Table 10](#) and [Table 11](#) show the dynamic modulus of the wearing course and base course, respectively. The mechanical properties

**Table 9**  
Detail traffic volume input.

Property	Phase I	Phase II
AADTT (veh/day)	4248	9913
Number of lanes	2	2
Operational speed (mph)	75	75

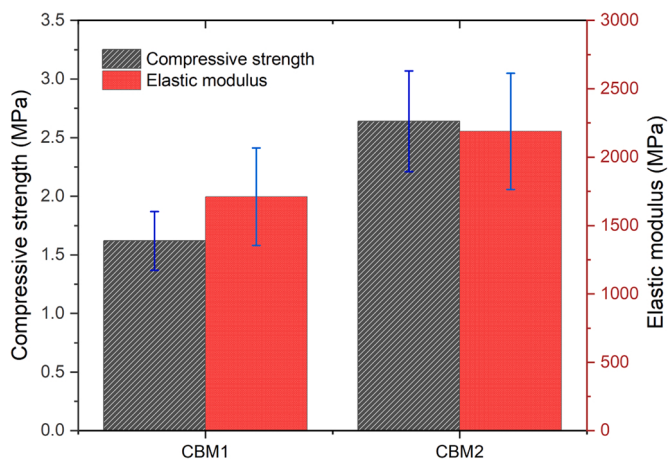


**Fig. 5.** Compressive strength and elastic modulus of CBM.

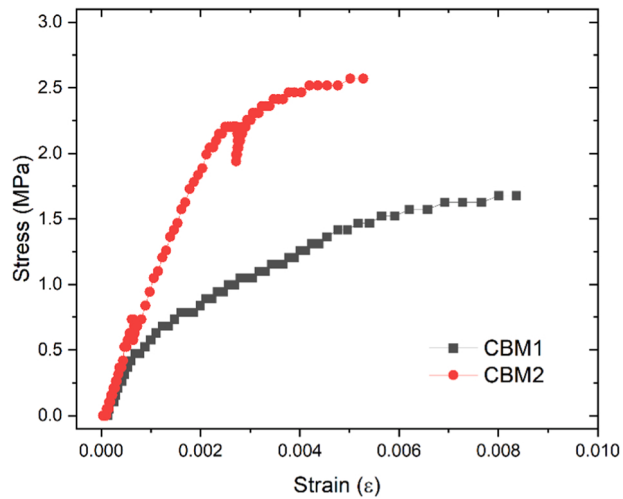


**Fig. 6.** Stress-strain behavior.

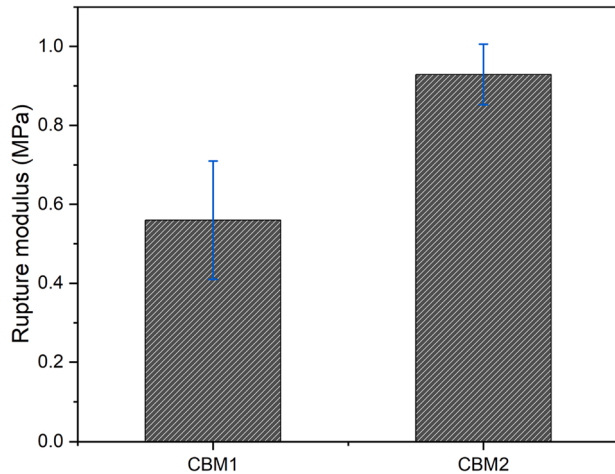


**Fig. 7.** Rupture modulus of CBM.

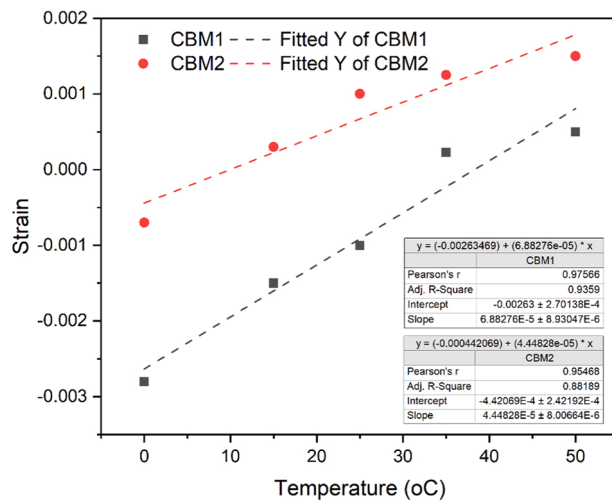


Fig. 8. CTE results of CBM mixture.

**Table 10**

Dynamic modulus of wearing course mixture (MPa).

Temperature (°C)	Frequency (Hz)					0.5	0.1
	25	10	5	1			
-10	33,386	32,024	30,137	27,736	26,436	22,623	
4	15,428	13,255	11,904	9844	8586	6884	
21	7785	6645	5345	3784	3136	2067	
37	4473	3203	2446	1352	1051	654	
54	2077	1,361	937	463	246	108	

**Table 11**

Dynamic modulus of base coarse mixture (MPa).

Temperature (°C)	Frequency (Hz)					0.5	0.1
	25	10	5	1			
-10	34,804	33,954	32,822	30,023	28,737	25,787	
4	27,449	25,820	24,502	20,818	19,304	15,497	
21	13,691	11361	9670	6162	4928	2846	
37	3132	2385	1875	1300	944	640	
54	1843	994	689	438	306	193	

of asphalt are influenced by its basic performance, aggregate gradation, and design properties of the mixture [36]. As observed in the table the dynamic modulus of the asphalt mixture increases with higher loading frequencies due to its viscoelastic nature. Under dynamic loading, the strength and modulus of the asphalt mixture are higher compared to static loading conditions, and this effect becomes more pronounced with increasing loading frequency [37]. Notably, the dynamic modulus of the asphalt mixture experiences a significant increase between 0.1 and 1 Hz, followed by a decrease between 5 and 25 Hz. This behavior is attributed to the asphalt mixture's higher elastic at high load frequencies, indicating that frequency has less influence on dynamic modulus compared to material properties.

Furthermore, the dynamic modulus of the asphalt mixture decreases as the temperature rises, primarily due to its sensitivity to temperature. At higher temperatures, the asphalt characteristics soften, resulting in decreased strength and stiffness, leading to a reduction in dynamic modulus [37]. As depicted in Table 11, the base course exhibits higher results in dynamic modulus compared to the wearing course. The base course is designed to distribute traffic and environmental loading, necessitating higher stiffness and adequate fatigue resistance compared to the wearing course.

### 3.5. Flow number

Fig. 9 illustrates the output of the flow number test. The curve depicts accumulated permanent deformation against the number of loading cycles, providing insight into the rutting resistance of mixtures. Flow number was found influenced by the viscosity of the binder, test temperature, effective binder content, and air voids. From the graph, it can be observed that the wearing course exhibits a

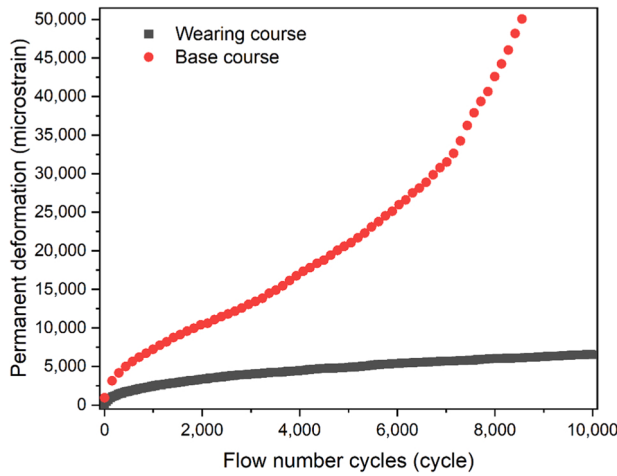


Fig. 9. Flow number of wearing course and base course.

higher number of loading cycles compared to the base course. The tertiary flow behavior indicates that the permanent deformation rate increases with loading. Thus, based on Fig. 9, the wearing course is more likely to endure more loading repetitions and exhibits less susceptibility to rutting compared to the base course. This behavior may occur due to variations in binders. The difference in binders employed in the course can explain this phenomenon. In comparison with the wearing course, the base course with asphalt binder PG 70-10 is noted to demonstrate more stiffness than the wearing course with PG 76-10. Due to the difference rheological properties, the two course behave differently. Flow number performance and behavior of each course are influenced by this disparity in binder characteristics.

### 3.6. Overlay test

Fig. 10 depicts the number of Overlay Test (OT) cycles at a specific load drop, highlighting the dominance of the wearing course with 454 OT cycles compared to the base course, which achieved 240 OT cycles at an 85 % load drop. The higher number of OT cycles in the wearing course suggests superior cracking resistance, while the lower number indicates faster crack propagation. Laboratory findings [38] indicate that stiffer mixes typically exhibit lower OT cycles, while softer mixes show higher OT cycles under similar test conditions. Additionally, softer mixes with higher OT cycles have generally demonstrated better cracking resistance in the field, although this relationship may be influenced by factors like sample air voids, pavement structure, construction, traffic levels, and climate.

Fig. 11 illustrates the correlation between percentage load drop and OT cycles. Generally, the load drop increased with the rise in repeated OT cycles. However, the base course exhibited a higher percentage of load drop compared to the wearing course. This phenomenon could be attributed to the different binder content between the two layers. Wearing course mixtures with higher binder

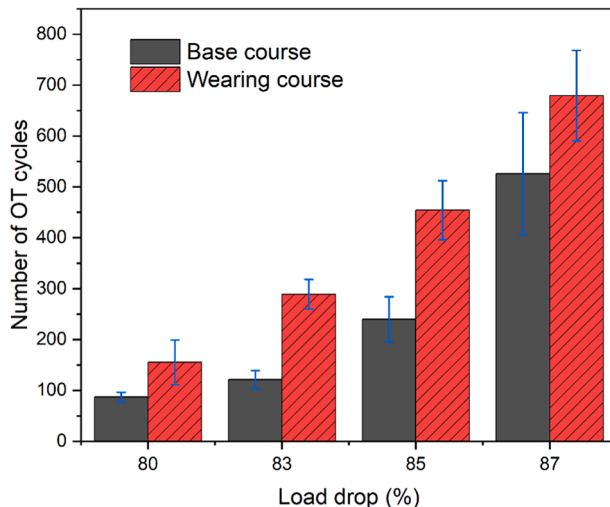


Fig. 10. Number of OT cycles.

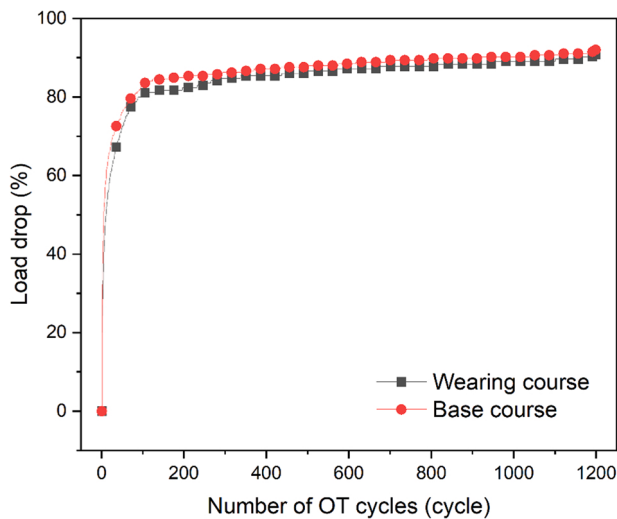


Fig. 11. Relationship between load drop and OT cycles.

content contribute to improved stiffness, resulting in better resistance to cracking. Meanwhile, the base course mixture, with lower binder content, may be more brittle, leading to a dramatic increase in load drop during the OT test process.

### 3.7. Subbase and subgrade

Table 12 presents the resilient modulus of the subbase and subgrade materials. The subbase material exhibits a higher resilient modulus than the subgrade material, possibly due to differences in material angularity. As deviatoric stress increases at each confining stress level, the strain also increases for both materials, indicating their deformation behavior under varying stress conditions. Specifically, the subbase material demonstrates an average resilient modulus of 196.44 MPa with COV (Coefficient of Variance) of 6.5 %, while the subgrade material shows an average resilient modulus of 92.02 MPa with COV of 13.1 %.

### 3.8. Pavement design

Table 13 provides a summary of predicted distresses for the Phase I pavement design. Among the cement-stabilized base designs, top-down cracking was the predominant form of fatigue cracking due to the robust base support minimizing bottom-up cracking [39]. Notably, despite CBM2 exhibiting higher elastic and rupture moduli in laboratory tests, the design analysis indicated elevated levels of AC total fatigue cracking and AC total transverse cracking for CBM2 compared to CBM1. This aligns with George's theory [40], suggesting that increased cement content correlates with heightened cracking. Predicted distress types, including terminal IRI (International Roughness Index) and total permanent deformation, followed a similar trend, with CBM2 exhibiting higher values than CBM1. Fig. 12 illustrates the total transverse cracking for both designs over 6 years of service. While both CBM1 and CBM2 met the requirement of total transverse cracking below 473.49, CBM1 demonstrated a lower value of 400.19 compared to CBM2's 403.38. As previously mentioned, higher cement content may contribute to increased cracking due to shrinkage during the hydration process. In conclusion, the findings emphasize the significant role of cement content in the propagation of cracking, particularly in transverse cracking throughout the pavement's service life.

Table 14 presents the Phase II design results. In contrast to Phase I, Case 2 with CBM2 exhibit lower total transverse cracking on the AC compared to Case 1 with CBM1. An increase in total transverse cracking may occur because of elevated vehicle volume, particularly when the asphalt binder undergoes hardening due to low temperatures. However, apart from AC total transverse cracking, Case 1 with CBM1 consistently demonstrated better performance than Case 2. As seen in Fig. 13, both Case 1 and Case 2 satisfied the design lifetime target of over 14 years. Considering the result from Phase I, which highlights that pavement constructed with cement stabilized layers are most susceptible to transverse cracking and block cracking, it is recommended to use pavement design with CBM1 for the connecting road between Al Faw Grand Port and Um Qasr in Iraq. Table 15 displays the Case 1 subgrade modulus parametric study, showing that the parameter of 0.95 M<sub>R</sub> resulted in the lowest distress, while the parameter of 0.80 M<sub>R</sub> resulted in the highest distress.

Table 12

Resilient modulus of subbase and subgrade.

Mixture	Average resilient modulus (MPa)	Standard deviation (MPa)	Coefficient of variance (%)
Subbase	196.4	12.8	6.5
Subgrade	92.0	12.1	13.1

**Table 13**

Phase I results of pavement design.

Distress type	Criteria	Retained percentage (%)	
		Case 1	Case 2
Terminal IRI (m/km)	2.72	1.99	2.01
Permanent deformation total (m)	0.013	0.0112	0.0115
AC total fatigue cracking (% lane area)	25.00	0.55	0.56
AC total transverse cracking (m/km)	473.49	400.19	403.38
AC bottom-up fatigue cracking (% lane area)	25.00	0.00	0.00
AC thermal cracking (m/km)	378.79	271.27	273.83
AC top-down fatigue cracking (% lane area)	25.00	8.58	8.58
Permanent deformation – AC only (m)	0.0064	0.0046	0.0046
Chemically stabilized layer (% lane area)	25.00	0.40	0.85
Performance life	6 years	> 14 years	> 14 years

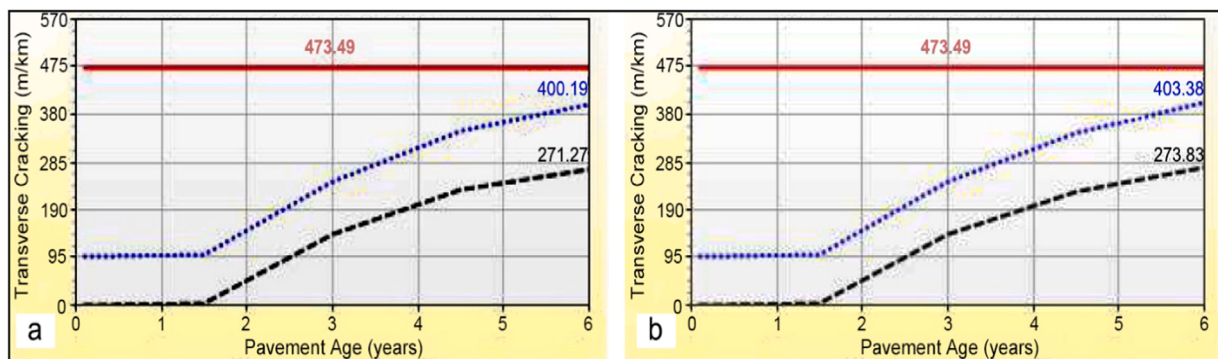


Fig. 12. Phase I AC total transverse cracking of (a) Case 1 and (b) Case 2.

**Table 14**

Phase II results of pavement design.

Distress type	Criteria	Retained percentage (%)	
		Case 1	Case 2
Terminal IRI (m/km)	2.72	2.03	2.03
Permanent deformation total (m)	0.013	0.0046	0.0048
AC total fatigue cracking (% lane area)	25.00	2.43	3.00
AC total transverse cracking (m/km)	473.49	471.53	470.21
AC bottom-up fatigue cracking (% lane area)	25.00	0.00	0.00
AC thermal cracking (m/km)	378.79	282	282
AC top-down fatigue cracking (% lane area)	25.00	10.49	10.49
Permanent deformation – AC only (m)	0.0064	0.0043	0.0043
Chemically stabilized layer (% lane area)	25.00	0.91	1.50
Performance life	14 years	> 14 years	> 14 years

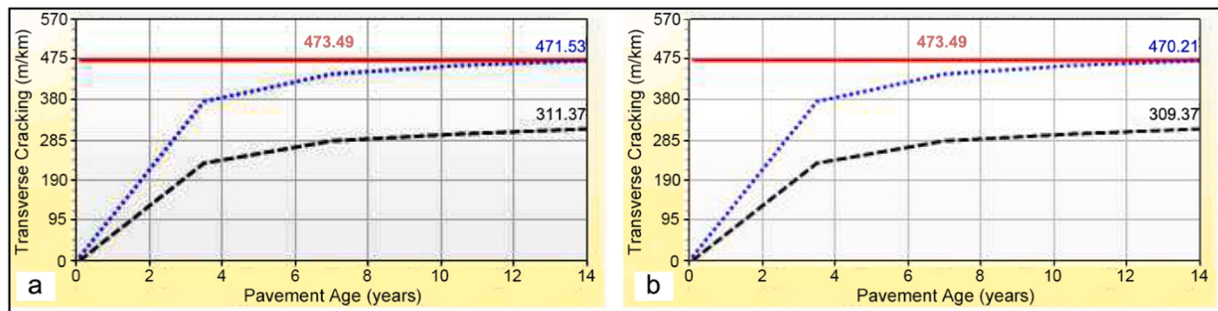


Fig. 13. Phase II AC total transverse cracking of (a) Case 1 and (b) Case 2.

**Table 15**

Case 1 subgrade modulus parameterized results.

Distress type	Criteria	Retained Percentage (%)			
		0.95 M <sub>R</sub>	0.90 M <sub>R</sub>	0.85 M <sub>R</sub>	0.80 M <sub>R</sub>
<b>PHASE I</b>					
Terminal IRI (m/km)	2.72	1.97	1.97	1.98	1.98
Permanent deformation total (m)	0.013	0.0104	0.0104	0.0106	0.0109
AC total fatigue cracking (% lane area)	25.00	0.55	0.55	0.55	0.55
AC total transverse cracking (m/km)	473.49	399.21	399.61	399.92	400.11
AC bottom-up fatigue cracking (% lane area)	25.00	0.00	0.00	0.00	0.00
AC thermal cracking (m/km)	378.79	262	262	262	262
AC top-down fatigue cracking (% lane area)	25.00	8.58	8.58	8.58	8.58
Permanent deformation – AC only (m)	0.0064	0.0046	0.0046	0.0046	0.0046
Chemically stabilized layer (% lane area)	25.00	0.34	0.35	0.36	0.38
<b>PHASE II</b>					
Terminal IRI (m/km)	2.72	2.02	2.02	2.03	2.03
Permanent deformation total (m)	0.013	0.0041	0.0043	0.0043	0.0045
AC total fatigue cracking (% lane area)	25.00	2.35	2.37	2.39	2.41
AC total transverse cracking (m/km)	473.49	470.55	470.95	471.26	471.45
AC bottom-up fatigue cracking (% lane area)	25.00	0.00	0.00	0.00	0.00
AC thermal cracking (m/km)	378.79	282	282	282	282
AC top-down fatigue cracking (% lane area)	25.00	10.49	10.49	10.49	10.49
Permanent deformation – AC only (m)	0.0064	0.0043	0.0043	0.0043	0.0043
Chemically stabilized layer (% lane area)	25.00	0.82	0.83	0.86	0.88

among the various parameters. The subgrade modulus may contribute to the occurrence of total transverse cracking in asphalt concrete (AC). An increase in the subgrade modulus can improve resistance to transverse cracking. For effective use of the subgrade parametric study, field conditions, such as weather and surrounding environmental conditions, should be taken into consideration.

#### 4. Conclusions

The current study aims to evaluate the effect of cement content on reflective cracking of asphalt pavement construct with Cement Base Material (CBM). Several laboratory tests were conducted to determine the performance of CBM, including elastic modulus, rupture modulus, and coefficient of thermal expansion. Meanwhile, dynamic modulus, overlay test, and flow number test were employed to find the properties of asphalt mixture for surface course and base course. The outcomes from experiments were used to calculate the performance life of pavement constructed with cement base materials by AASHTOWare Pavement ME Design program. Several key findings have been drawn as follows:

- In laboratory tests, CBM2, featuring higher cement content than CBM1, showcased superior mechanical properties, displaying elevated elastic modulus (2189 MPa) and rupture modulus (0.929 MPa). This suggests increased rigidity and strength attributable to higher cement levels and differences in aggregate proportions.
- The coefficient of thermal expansion (CTE) in CBM1 with 4.5 % cement content exhibited lower strains compared to CBM2 with 5.4 % cement content, indicating a decrease in CTE as cement content decreased.
- Based on laboratory experiments and the AASHTOWare Pavement ME Design program, it was observed that CBM with a lower cement content (4.5 %) exhibited enhanced performance in cracking resistance, particularly in total transverse cracking.
- It can be concluded that the cement content of CBM plays a significant role in pavement cracking. Within the context of this study, a 4.5 % cement content provided more effective in resisting cracking compared to 5.4 %.

In summary, this study evaluates cement contents impact the properties of cement bound material and the occurrence of reflective cracking in asphalt pavement. Although several key findings have been found, it is recommended to monitor reflective cracking after several years of service to confirm the design's long-term effectiveness in future research.

#### CRediT authorship contribution statement

**Dae-Wook Park:** Writing – review & editing, Supervision, Project administration, Conceptualization. **Dong-Wook Lee:** Writing – original draft, Validation, Methodology, Data curation. **Tam Minh Phan:** Writing – review & editing, Writing – original draft, Software, Methodology, Formal analysis, Data curation, Conceptualization. **Debby Marcelia Andryanti:** Writing – review & editing, Writing – original draft, Validation, Formal analysis, Data curation.

#### Declaration of Competing Interest

The authors whose names are listed immediately below certify that they have NO affiliations with or involvement in any organization or entity with any financial interest or non-financial interest in the subject matter or materials discussed in this manuscript.

## Data availability

Data will be made available on request.

## Acknowledgment

This work was supported by the National Research Foundation of Korea (NRF) grant funded by the Korea government (MSIT) (No. 2022R1F1A1063979).

## Conflicts of interest

None.

## References

- [1] M.A.A. A, H.E. T, V.M.F.C. van de, Effects of aging on the mechanical characteristics of bituminous binders in PAC, *J. Mater. Civ. Eng.* 22 (2010) 779–787, [https://doi.org/10.1061/\(ASCE\)MT.1943-5533.0000021](https://doi.org/10.1061/(ASCE)MT.1943-5533.0000021).
- [2] Z. Dong, F. Ni, Dynamic model and criteria indices of semi-rigid base asphalt pavement, *Int. J. Pavement Eng.* 15 (2014) 854–866, <https://doi.org/10.1080/10298436.2014.893322>.
- [3] G.E. Halsted, D.R. Luhr, W.S. Adaska, Guide to cement-treated base (CTB), 2006.
- [4] P. Tataranni, C. Sangiorgi, A. Simone, V. Vignali, C. Lantieri, G. Dondi, A laboratory and field study on 100 % recycled cement bound mixture for base layers, *Int. J. Pavement Res. Technol.* 11 (2018) 427–434, <https://doi.org/10.1016/j.ijprt.2017.11.005>.
- [5] K.E. Hassan, O. El-Hussain, M. bin-S. Al-Kuwari, K. Al-Emadi, Development and performance of cement bound materials in road pavements, in: *Proc. Int. Conf. Civ. Infrastruct. Constr.* 2020, 2020, pp. 553–9. (<https://doi.org/10.29117/cic.2020.0069>).
- [6] W. Zhang, S. Shen, P. Basak, H. Wen, S. Wu, A. Faheem, L.N. Mohammad, Development of predictive models for initiation and propagation of field transverse cracking, *Transp. Res.* 2524 (2015) 92–99, <https://doi.org/10.3141/2524-09>.
- [7] Y.H. Huang, *Pavement Analysis and Design*, Pearson Prentice Hall, Upper Saddle River, NJ, 2004.
- [8] S. Werkmeister, Copyright ASCE 2006 126 Pavement Mechanics and Performance (GSP 154) Pavement Mechanics and Performance, 2006, pp. 126–33.
- [9] I. Gilbert, Shrinkage, cracking and deflection—the serviceability of concrete structures, *Electron. J. Struct. Eng.* 1 (2001) 15–37.
- [10] K. Kovler, S. Zhutovsky, Overview and future trends of shrinkage research, *Mater. Struct. Constr.* 39 (2006) 827–847, <https://doi.org/10.1617/s11527-006-9114-z>.
- [11] D.T. Davidson, Soil Stabilization with Portland Cement, Highway Research Board Bulletin, Natl. Acad. Sci. Washington, DC, USA, 1961.
- [12] X. Lan, X. Zhang, Z. Hao, Y. Wang, Strength and shrinkage properties of cement stabilized macadam bases incorporating 0–2.36 millimetre recycled fine aggregate, *Case Stud. Constr. Mater.* 16 (2022) e00984.
- [13] L. Titus-Glover, B.B. Bhattacharya, D. Raghunathan, J. Mallela, R.L. Lytton, Adaptation of NCHRP project 1-41 reflection cracking models for semirigid pavement design in AASHTOWare pavement ME design, *Transp. Res. Rec.* 2590 (2016) 122–131.
- [14] B. Yu, Q. Lu, J. Yang, Evaluation of anti-reflective cracking measures by laboratory test, *Int. J. Pavement Eng.* 14 (2013) 553–560.
- [15] ASTM C39, Standard Test Method for Compressive Strength of Cylindrical Concrete Specimens 1, ASTM Int. i (2005) 1–7.
- [16] British Standards Institution, Methods of test for soils for civil engineering purposes — Part 4, Br. Stand., 1975, pp. 1–28
- [17] C. ASTM, Standard test method for flexural strength of concrete (using simple beam with third-point loading), in: Am. Soc. Test. Mater., ASTM Michigan, United States, 2010, pp. 12959–9428.
- [18] AASHTO T342-11, Standard Method of Test for Determining Dynamic Modulus of Hot Mix Asphalt (HMA) | GlobalSpec, American Association of State Highway and Transportation Officials, 2009
- [19] TEX-248-F, TEX-248-F, Overlay Test, Constr. Div. Texas Dep. Transp., 2009
- [20] T. Bennert, Dynamic Modulus of Hot Mix Asphalt, 2009.
- [21] K.E. Kaloush, Simple Performance Test for Permanent Deformation Evaluation of Asphalt Mixtures, Arizona State University, 2006. (<https://doi.org/10.1617/2912143772.062>).
- [22] F. Zhou, T. Scullion, Upgraded Overlay Tester and Its Application to Characterize Reflection Cracking Resistance of Asphalt Mixtures (No. FHWA/TX-04-0-4467-1), Texas Transportation Institute, Texas A & M University System, 2003.
- [23] F. Zhou, S. Hu, X. Hu, T. Scullion, M. Mikhail, L.F. Walubita, Development, calibration, and verification of a new mechanistic-empirical reflective cracking model for HMA overlay thickness design and analysis, *J. Transp. Eng.* 136 (2010) 353–369.
- [24] F. Zhou, T. Scullion, Overlay Tester: A Rapid Performance Related Crack Resistance Test (FHWA/TX-05-0-4467-2), Texas Transportation Institute, College Station, 2005, Citeseer, 2005.
- [25] AASHTO-T307, Standard Method of Test for Determining the Resilient Modulus of Soils and Aggregate Materials Standard Method of Test for of Soils and Aggregate Materials, vol. 99, 2012, pp. 0–42
- [26] AASHTOWare, AASHTOWare Pavement ME Design Manual of Practice, Am. Assoc. State Hwyw. Transp. Off. Washington, DC, 2022
- [27] J. Saha, S. Nassiri, A. Bayat, H. Soleymani, Evaluation of the effects of Canadian climate conditions on the MEPDG predictions for flexible pavement performance, *Int. J. Pavement Eng.* 15 (2014) 392–401, <https://doi.org/10.1080/10298436.2012.752488>.
- [28] K. Hanifa, M.Y. Abu-Farsakh, G.P. Gautreau, Design Values of Resilient Modulus for Stabilized and Non-Stabilized Base, Louisiana Transportation Research Center, 2015.
- [29] R. Wassermann, A. Katz, A. Bentur, Minimum cement content requirements: a must or a myth? *Mater. Struct.* 42 (2009) 973–982.
- [30] S. Pongsivashit, S. Horipibulsuk, S. Piayaphipat, Assessment of mechanical properties of cement stabilized soils, *Case Stud. Constr. Mater.* 11 (2019) e00301.
- [31] B.L. Karihaloo, H.M. Abdalla, Q.Z. Xiao, Size effect in concrete beams, *Eng. Fract. Mech.* 70 (2003) 979–993.
- [32] M. Ahmed, J. Mallick, M.A. Hasan, A study of factors affecting the flexural tensile strength of concrete, *J. King Saud. Univ. Sci.* 28 (2016) 147–156.
- [33] M.S. Siddiqui, D.W. Fowler, A systematic optimization technique for the coefficient of thermal expansion of Portland cement concrete, *Constr. Build. Mater.* 88 (2015) 204–211.
- [34] J. Mallela, A. Abbas, T. Harman, C. Rao, R. Liu, M.I. Darter, Measurement and significance of the coefficient of thermal expansion of concrete in rigid pavement design, *Transp. Res. Rec.* 1919 (2005) 38–46.
- [35] J. Tanesi, M.E. Kutay, A. Abbas, R. Meininger, Effect of coefficient of thermal expansion test variability on concrete pavement performance as predicted by mechanistic-empirical pavement design guide, *Transp. Res. Rec.* 2020 (2007) 40–44.
- [36] O.C. Assogba, Y. Tan, Z. Sun, N. Lushingza, Z. Bin, Effect of vehicle speed and overload on dynamic response of semi-rigid base asphalt pavement, *Road Mater. Pavement Des.* 22 (2021) 572–602, <https://doi.org/10.1080/14680629.2019.1614970>.
- [37] P. Li, M. Zheng, F. Wang, F. Che, H. Li, Q. Ma, Y. Wang, Laboratory performance evaluation of high modulus asphalt concrete modified with different additives, *Adv. Mater. Sci. Eng.* 2017 (2017).

- [38] L.F. Walubita, J. Hoeffner, T. Scullion, FHWA/TX-13/0-6132-3: New Generation Mix-Designs: Laboratory-Field Testing and Modifications to Texas HMA Mix-Design Procedures, Texas, Dept. of Transportation. Research and Technology Implementation Office, 2013.
- [39] Y. Zhao, M. Alae, G. Fu, Investigation of mechanisms of top-down fatigue cracking of asphalt pavement, *Road Mater. Pavement Des.* 19 (2018) 1436–1447.
- [40] K. George, Shrinkage characteristics of soil-cement mixtures, *Highw. Res. Rec.* 255 (1968) 42–57 (No. 255).